2014

Inference of strata separation and gas emission paths in longwall overburden using continuous wavelet transform of well logs and geostatistical simulation

C. Ozgen Karacan
NIOSH, Office of Mine Safety and Health Research

Ricardo A. Olea
USGS, Eastern Energy Resources

Journal of Applied Geophysics 105 (2014) 147–158

Contents lists available at ScienceDirect

Journal of Applied Geophysics

journal homepage: www.elsevier.com/locate/jappgeo

Inference of strata separation and gas emission paths in longwall overburden using continuous wavelet transform of well logs and geostatistical simulation

C. Özgen Karacan [a,*], Ricardo A. Olea [b]

[a] NIOSH, Office of Mine Safety and Health Research, Pittsburgh, PA, United States
[b] USGS, Eastern Energy Resources, Reston, VA, United States

ARTICLE INFO

Article history:
Received 28 October 2013
Accepted 25 March 2014
Available online 1 April 2014

Keywords:
Strata separation
Longwall mining
Methane flow paths
Wavelet transform
Geostatistical simulation

ABSTRACT

Prediction of potential methane emission pathways from various sources into active mine workings or sealed gobs from longwall overburden is important for controlling methane and for improving mining safety. The aim of this paper is to infer strata separation intervals and thus gas emission pathways from standard well log data. The proposed technique was applied to well logs acquired through the Mary Lee/Blue Creek coal seam of the Upper Pottsville Formation in the Black Warrior Basin, Alabama, using well logs from a series of boreholes aligned along a nearly linear profile.

For this purpose, continuous wavelet transform (CWT) of digitized gamma well logs was performed by using Mexican hat and Morlet, as the mother wavelets, to identify potential discontinuities in the signal. Pointwise Hölder exponents (PHE) of gamma logs were also computed using the generalized quadratic variations (GQV) method to identify the location and strength of singularities of well log signals as a complementary analysis. PHEs and wavelet coefficients were analyzed to find the locations of singularities along the logs.

Using the well logs in this study, locations of predicted singularities were used as indicators in single normal equation simulation (SNESIM) to generate equi-probable realizations of potential strata separation intervals. Horizontal and vertical variograms of realizations were then analyzed and compared with those of indicator data and training image (TI) data using the Kruskal–Wallis test. A sum of squared differences was employed to select the most probable realization representing the locations of potential strata separations and methane flow paths.

Results indicated that singularities located in well log signals reliably correlated with strata transitions or discontinuities within the strata. Geostatistical simulation of these discontinuities provided information about the location and extents of the continuous channels that may form during mining. If there is a gas source within their zone of influence, paths may develop and allow methane movement towards sealed or active gobs under pressure differentials. Knowledge gained from this research will better prepare mine operations for potential methane inflows, thus improving mine safety.

Published by Elsevier B.V.

1. Introduction

Stress-relief fractures that occur during longwall mining provide extensive pathways for gas migration from gas-bearing strata or environments with accumulations of methane—such as abandoned workings, uncased shafts, or wellbores—into sealed and active areas. Due to high conductivity of bedding plane separations, methane emissions can occur suddenly with large gas quantities inundating the ventilation system and changing the properties of the mine atmosphere over large areas. To evaluate the likelihood of methane migrations from different sources into the sealed and active gobs, and to effectively control methane in the overburden, it is important to estimate intervals of strata separations and to identify paths that these emissions may follow.

The presence of mining-induced bedding plane separations has important implications beyond ground control objectives; these fractures generally have very high conductivity for fluid flow, as demonstrated by Karacan et al. (2007) and Karacan and Goodman (2009). Well test analyses of gob gas venthole production showed that average permeabilities in the fractured zone of gob may vary between 1000 and 15,000 millidarcies (md) (Karacan, 2009a). The author noted, however, that the properties of individual heterogeneities were all lumped together in this analysis to represent an effective average since analyzed flow came from a long interval of the gob. Therefore, permeability of individual fractures may be even higher. Later, Karacan and Goodman (2011) conducted further work by studying measured casing strain

* Corresponding author.

http://dx.doi.org/10.1016/j.jappgeo.2014.03.019
0926-9851/Published by Elsevier B.V.

during mining and by analyzing production data during this period. They determined that one of the major strata separations could be as much as 0.55 ft with a permeability of ~80,000 md, while the effective average of the rest of the fractured gob interval could have permeability values of ~20,000 md. These are significant values for potential gas flow within the gob and between active and sealed portions of the mine, if strata separations and fractures intercept gas sources within the zone affected from the mining stresses. Therefore, the ability to predict strata separation intervals is critical in this zone for effective control of methane gas in underground coal mining operations.

Existing methods to locate intervals of strata separations rely on empirical and numerical methods. An empirical method proposed by Palchik (2003, 2005) is based on the correlation of the presence and absence of estimated horizontal fractures with uniaxial compressive strength and thickness of rock layers, distances from the extracted coal seam to the rock layer interfaces, and the thicknesses of extracted coal. His observations on the existence of horizontal fractures at different overburden rock-layer interfaces indicate that the probability of fracturing increased with the compressive strength difference between neighboring rock layers. It should be noted that, according to these observations, not every strata interface—not even every one of the strong-weak rock interfaces—is prone to separation.

Numerical models, on the other hand, are mostly geomechanical models that require exhaustive data sets of strata and interface properties to produce accurate results. By using such models and input data sets Whittles et al. (2006) conducted studies on the effect of different geotechnical factors on characteristics of fracturing, gas sources, and gas flow paths for longwall operations in the United Kingdom. Gale (2005) simulated rock fracture, caving, stress redistribution, and induced hydraulic conductivity enhancements around longwall panels. He reported that the horizontal conductivity can be significantly enhanced along bedding planes within and outside the panel, thereby increasing the potential of methane migration from affected regions. Guo et al. (2012) monitored strata displacement, stress, and water pressure changes at longwall overburden, and modeled stress changes, permeability conditions, and gas flow dynamics.

Empirical or numerical approaches for determining intervals of strata separation are difficult, time consuming, and require highly dependable input data, which may or may not be readily available. In addition, these methods are deterministic, producing results that are absolute and without any room for uncertainty. In consideration of the significant permeability values that strata separations may have, it is correct to say that the ability to predict the intervals and uncertainties of strata separations can help not only to control and capture methane more effectively, but can also assess an imminent methane in-flow danger at an active mine.

The aim of this work is to infer strata separation intervals in longwall overburden by an alternative method that relies only on well logs as the input data and on signal processing and stochastic geostatistical simulation techniques. Well logs and geophysical techniques have been applied to address various issues related to oil and gas reservoirs, as well as coal mining (e.g., Hatherly, 2013; Karacan, 2009b and the references therein). Therefore, uses of well logs for conventional formation evaluation purposes will not be reviewed and repeated here. Instead, researchers will examine well logs, in particular the gamma log, from a signal interpretation and processing perspective, and will aim to model its singularities using geostatistical approaches to infer strata separation intervals with associated uncertainty.

2. Motivation, approach to the problem, and the general workflow

2.1. Motivation

The motivation behind this work is the premise that geological stratigraphic sequences contain localized weaknesses, either at the interfaces between formations or within formations due to inclusions or concentration of different layers of minerals. Such weaknesses, which may not be evident to geologists or engineers using conventional techniques, can create fractures, i.e. strata separations, under mining-induced stresses. Once these locations fail, they may prevent strata separation at other locations that at first glance are deemed better candidates for fracturing since stresses will be relieved at those weak locations. Therefore, locating and mapping these weaknesses with their spatial distribution can better predict intervals of strata separations that will occur under mining-induced stresses and can identify the resulting flow paths of strata gas.

Fortunately, the locations of strata weaknesses can manifest themselves by abrupt changes in magnitudes and/or frequencies of well log signals. These are termed singularities in signal processing language and are easily distinguished using localized amplitude-frequency analyses of well logs. These singularities can be the precursors for strata separations. Well logs are merely signals recorded as responses of geologic formations to various inputs, or signals that originate from various properties inherent to the formations along the boreholes. Moreover, they are nearly exact measures of relevant data with relatively high resolution along the axis of measurement. Therefore, putting them under a mathematical microscope to detect singularities may enable us to use well logs to predict intervals of strata separations to assist geomechanical models or empirical approaches.

2.2. Methodology and workflow

In this work, a profile that intercepted six boreholes along its horizontal length in the studied area within the Brookwood and Oak Grove coalbed methane fields in Alabama, USA, was selected. Gamma and density logs acquired in these boreholes are shown in Fig. 1. Continuous wavelet transform (CWT) was used to detect singularities in the gamma log data of the boreholes from their wavelet coefficient maps. In theory, if a wavelet is stronger in identifying locations, it is weaker for the identification of scales, and vice versa. For instance, the Morlet wavelet provides a better localization of frequencies that correspond to uniformities or singularities, whereas the Mexican hat wavelet provides a better location of the depths that correspond to those changes. In this work, both were utilized to take advantage of their specialized properties in locating singularities and scales at which they could be analyzed. As it will be shown in Section 4.2, scale 40 was found as the appropriate scale for identification of singularities from the wavelet coefficient maps. In the identification of this scale, the coefficients in the scalograms of Mexican hat and Morlet wavelets were analyzed together. The criterion was to mark the scale as the boundary where singularities actually showed up and continued to lower scale values with diminishing coefficients. Haar wavelet, which is a member of Daubechies wavelet family and is a special case known as D2, is another mother wavelet that is proposed for the purpose of identification of abrupt changes in signals (Perez-Muñoz et al., 2013). However, it has not been used in this work due to its discontinuous and thus non-differentiable nature.

Pointwise Hölder exponents (PHE), which are the measure of the strength of the singularities in a signal, were also determined using the generalized quadratic variation (GQV) method as complementary to the CWT analyses. In the GQV method of PHE computation around each log data, a gamma value of 0.7 with geometric sampling using a minimum of 1 and a maximum of 16 values were employed. Therefore, up to 16 values in the neighborhood of each data were used to generate a PHE for each data point. These parameters were used to generate approximately 1600 PHE in the neighborhood of approximately 1600 individual data points of each of the well logs.

Both CWT and PHE are used in hydrology (Gaucherel, 2002), in atmospheric sciences (Domingues et al., 2005), and in biomedical sciences (Humeau et al., 2007) among others. CWT and waveform analyses techniques, in particular, are used in oil fields for facies recognition (López and Aldana, 2007), stratigraphic identification of formation interfaces (Pan et al., 2008), multiscale analysis of log measurements (Briqueu

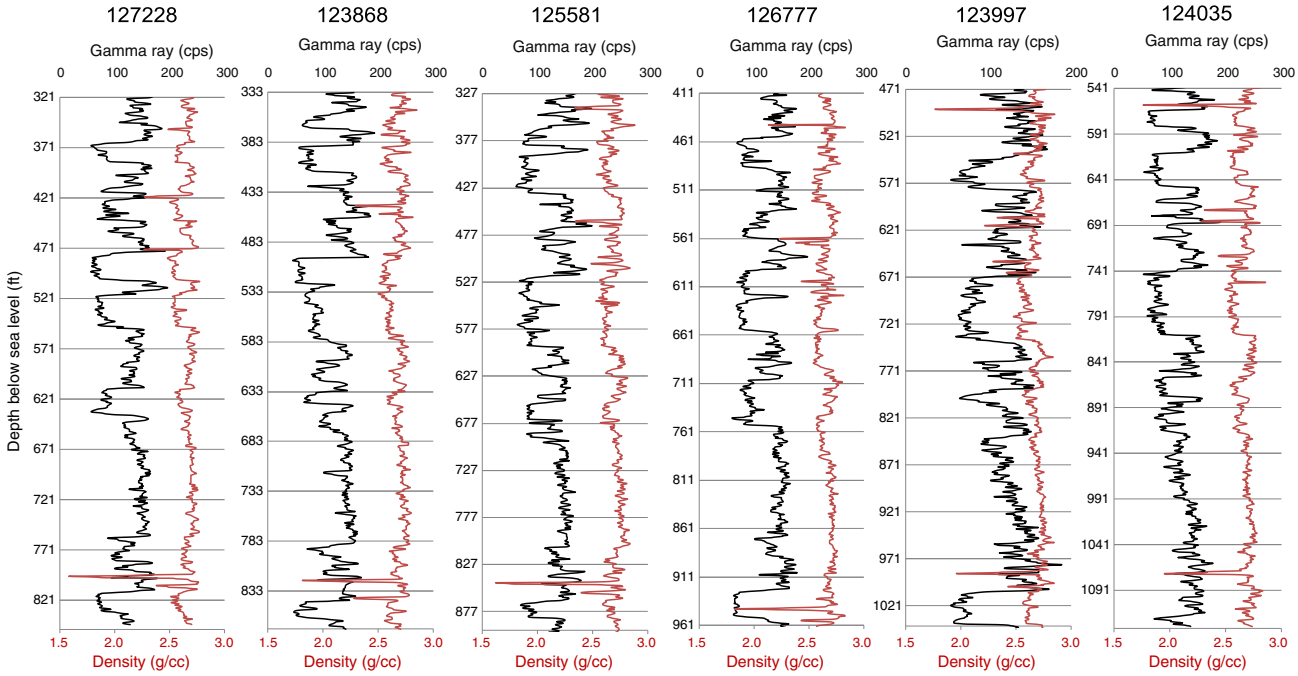

Fig. 1. Well logs digitized and studied in this work.

et al., 2010), and for lithological characterization of oil fields (Perez-Muñoz et al., 2013).

After analysis of wavelet coefficient maps, determined singularity locations were coded as "1" into the well log data, and the rest of the locations were coded with "0" following a classical indicator coding. Indicator coding has been covered in various papers related to indicator kriging or indicator simulation (e.g., Bastante et al., 2008; de Souza and Costa, 2013; Webber et al, 2013). Indicator data can be modeled, of course, for spatial correlation using semivariograms. However, since horizontal distances were too large for meaningful semivariograms, SNESIM formulation of SGeMS—Stanford Geostatistical Modeling Software— (Remy et al., 2009) along with a training image (TI) was used. The TI that is required for SNESIM application was produced by thresholding and binarizing the lithological cross section generated by CORRELATOR (Olea, 2004) from gamma and density logs of the same boreholes along the same profile selected for modeling. SNESIM generated 100 equi—probable realizations of the singularity maps across the vertical plane of the studied cross section, which were then interpreted as potential intervals of strata weaknesses, or separations, if exposed to mining-induced stresses.

Next, horizontal and vertical semivariograms of 100 realizations from SNESIM were determined and compared with those of the indicator data and the TI using the statistical Kruskal–Wallis test and using the sum of squared differences for comparison of distributions. These analyses not only helped in selecting the most likely strata weakness distribution that would satisfy the spatial properties of the TI and the indicator data, but also helped in the quantification of uncertainty.

Fig. 2 shows the methodology flowchart applied in this study and also the general structure of this paper to illustrate its main components. The performed study and results will be discussed in detail in upcoming sections.

3. Description of the study area

This study was conducted in the Brookwood and Oak Grove coalbed methane fields, located in the Black Warrior Basin, Alabama. Structural and geological properties of the Black Warrior Basin have been discussed extensively in Groshong and Pashin (2009) and in Pashin et al. (2010). Therefore, these aspects will not be repeated. However, it is worth mentioning that the coal-bearing strata of economic value from mining and gas production activities are in the Pennsylvanian-age Pottsville Formation. During coal mining, the Mary Lee and Blue Creek seams are usually mined together where the parting layer is thin. Therefore, they can be referred to as a single coal seam for mining purposes.

Coalbed methane in this field has been produced since the 1980s with vertical wells having multiple completions at the Pratt, Mary Lee, and Black Creek coal groups (Karacan, 2013a). These wells have also been logged extensively using gamma, density, resistivity, and caliper tools for locating completion intervals and identifying strata. Methane production using vertical wells resulted in reduction in gas-in-place of the coal seams of these coal groups, particularly in those that are of importance for gas emissions due to mining (Karacan and Olea, 2013). Active longwall coal mining has taken place for the last several years in the specific Mary Lee/Blue Creek seam study area (Fig. 3). Safe and productive mining of these seams necessitated further degasification 2–3 years in advance using horizontal wells (Karacan, 2013b).

As mining progressed into areas with active boreholes, the wells were terminated for production and casing was removed. Furthermore, as one of the consequences of longwall mining, overburden strata were deformed starting from the top of the Mary Lee coal seam, where the immediate roof is in the caved zone, and extending upwards close to the Pratt group seam. Therefore, the interval between the top of the Mary Lee seam to the bottom of Pratt seams can be considered within the zone of interest for evaluating potential strata separation locations.

Fig. 3 shows, on a surface elevation map, the general study area with locations of all vertical boreholes drilled for methane production and the vertical faults in the Pottsville formation. The profile connecting the six boreholes along which the work was conducted is shown as well. The length of the profile is 15,500 ft and the thickness of the stratigraphic interval of interest for modeling (between PR and ML—Fig. 4A) is about 700 ft.

4. Technical work, results, and discussion

4.1. Stratigraphic correlation

The stratigraphic correlation along the analysis profile shown in Fig. 3 was performed using CORRELATOR (Olea, 2004), which is a

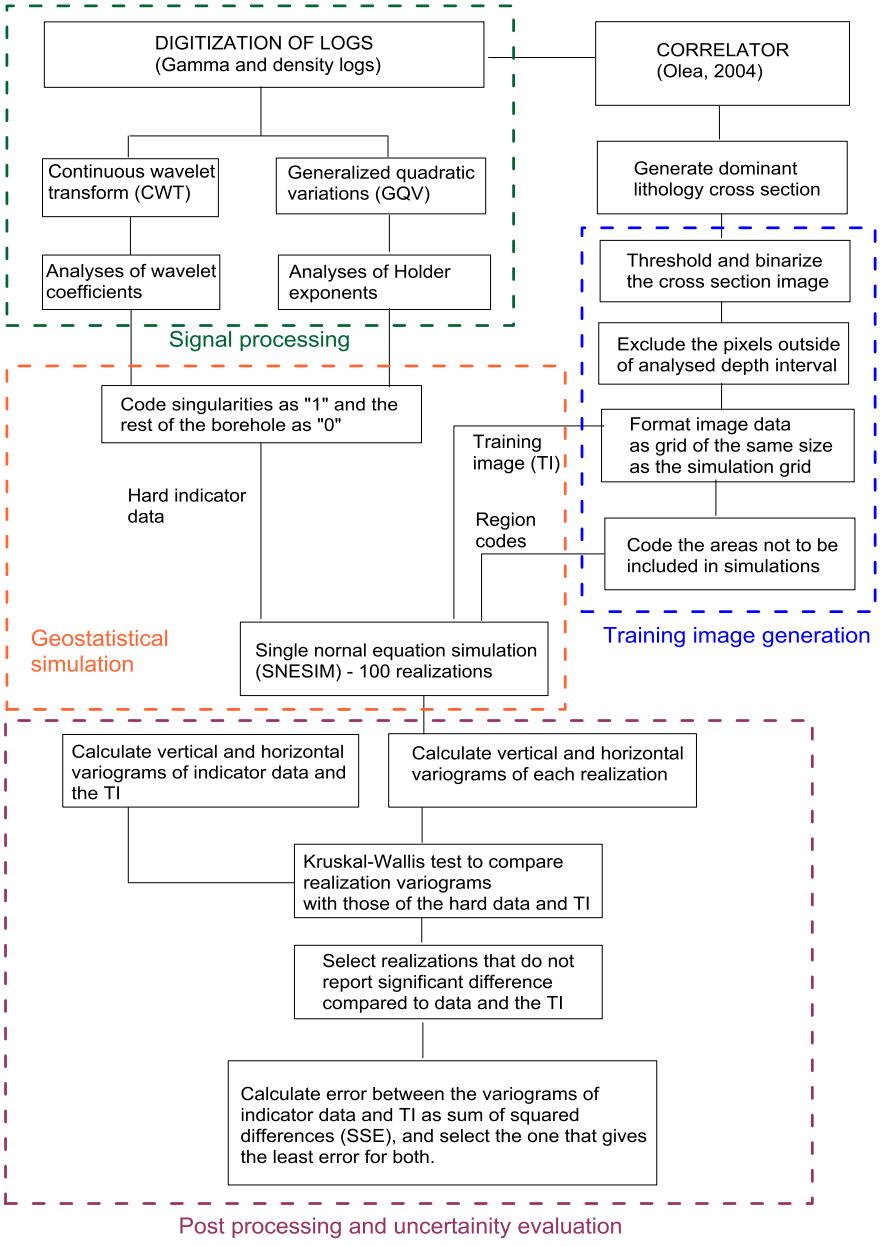

Fig. 2. General workflow and flowchart of the study methodology.

software for establishing lithostratigraphic correlations between logged intervals. CORRELATOR uses mathematical and statistical techniques for the determination of stratigraphic equivalence using simultaneous assessment of similarity in shale content, similarity in the patterns of vertical variation in a petro-physical property, and spatial consistency in stratigraphic relationships. Particularly, using weighted correlation provides an objective quantitative measure of the quality of matching for every equivalence (tie) line.

In order to generate the stratigraphic correlation along the profile shown in Fig. 3, the general procedure detailed in Olea (2004) was employed using gamma and density logs digitized in 0.5-ft intervals for each well. The depths of the logs were calibrated for sea level, which was used as datum in correlations. Fig. 4 shows the stratigraphic correlation produced by CORRELATOR between 127228 (6732-C) and 124035 (5730-C). Fig. 4-A shows the lithology log and shale content of 127228, with markings at the bottom of the Pratt group of seams (PR) and the top of the Mary Lee seam (ML)—the interval of interest for strata separations during mining and that will be used for singularity assessment and modeling. As the shale log shows, the strata are mainly composed of formations rich in shale with alternating continuous formations low in shale, such as sandstone, limestone, and coal. Fig. 4-B, on the other hand, is the cross section for major lithologies distinguished by shale content, and is generated between the six wells. The cutoff for this definition was 50% shale. The vertical scale was exaggerated 10 times in order to visualize the correlated layers and their continuity. The strata shown with yellow are the formations with shale less than 50%, and thus mostly sandstone and limestone. Gray layers are shale-rich formations, with coals shown in black.

The singularities that may occur along the depth interval in this area, either between the formations or within the formations, may be hidden in these correlated cross sections as data signatures of the logs, particularly of the gamma log due to its sensitivity to composition and type of rocks. Exploring these singularities and discussion of the employed techniques are the subject of the next section.

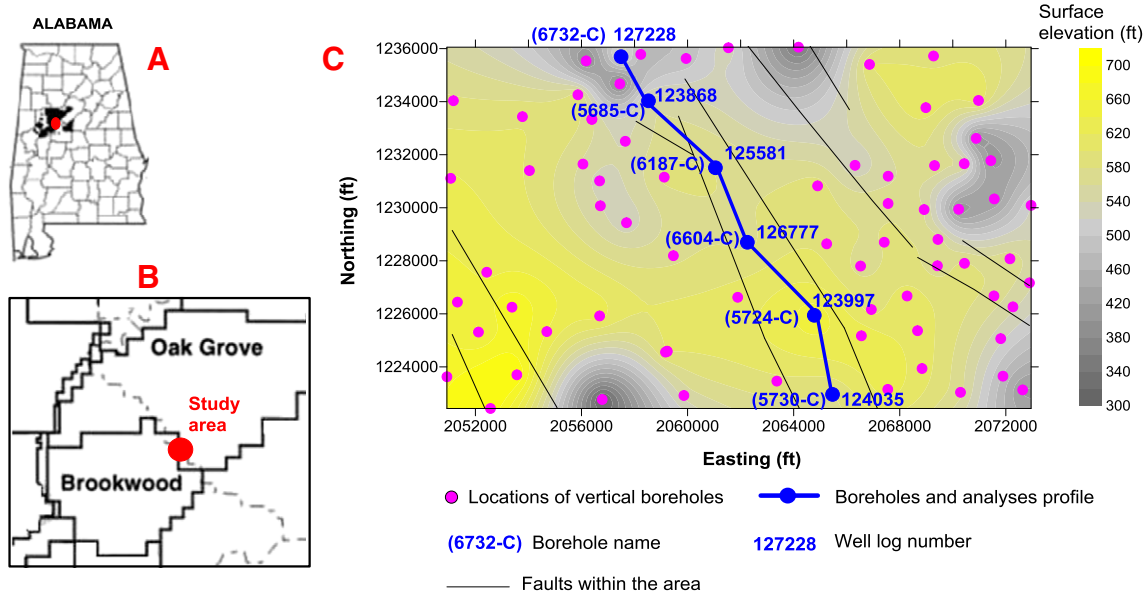

Fig. 3. Alabama and its coalbed methane fields with the approximate location of study area (A), location of the study area in Brookwood and Oak Grove fields (B), and surface elevation map of study area and specific wellbores along which stratigraphic cross sections were evaluated for potential strata separation intervals (C).

4.2. Analyses of well logs using continuous wavelet transform (CWT) and Hölder exponents

Continuous wavelet transform (CWT) can be considered as a mathematical microscope and is proven to be very useful for scanning the singularities in a signal, either in time or in a coordinate of measurement, such as depth. The singularities in the signal are abrupt changes in the magnitude or frequency of the signal and can be associated with changes in events that dictate a system's behavior or uniformity of the collected data. Examples from the applications of CWT were given in Section 2. However, it is important to note that the singularities may or may not be evident for macroscopic detection. CWT is

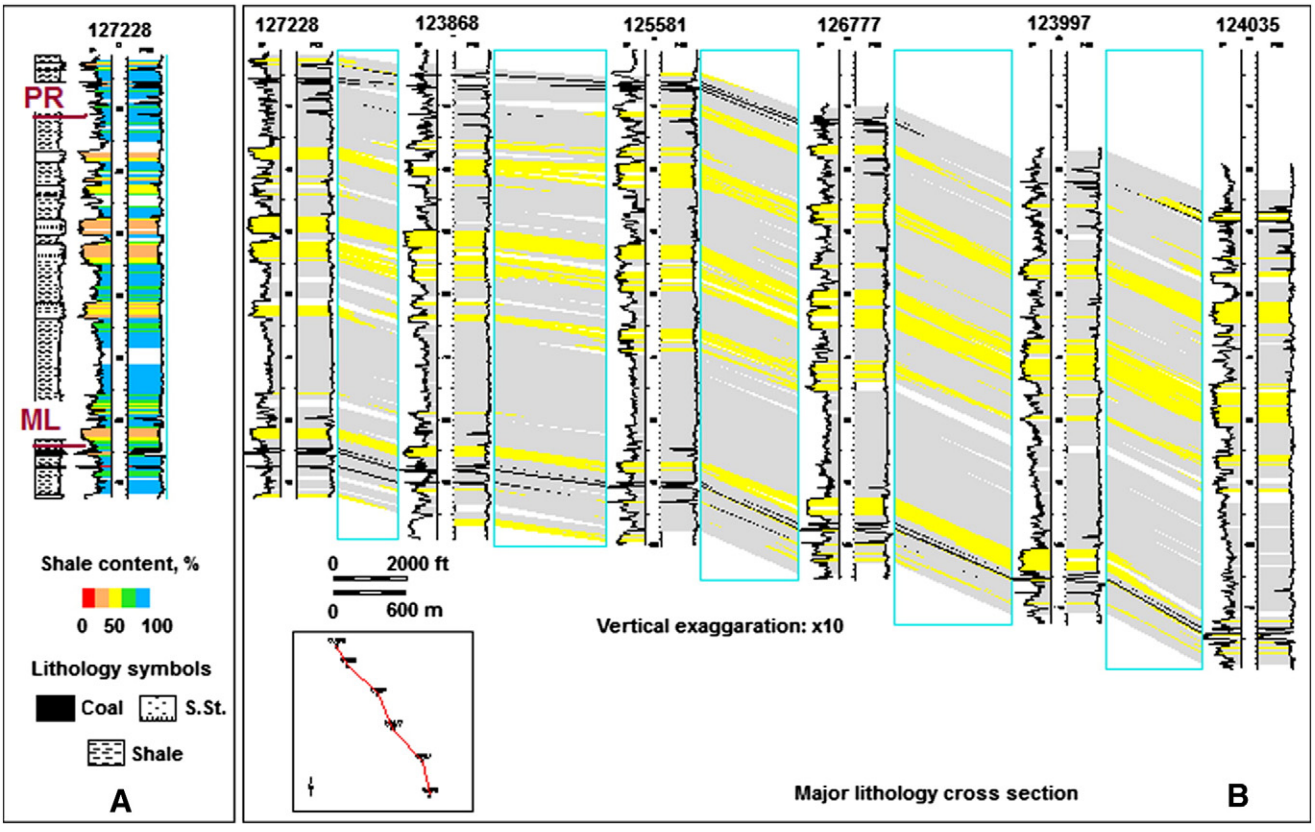

Fig. 4. CORRELATOR-generated stratigraphic correlations between six wells along the profile shown in Fig. 3. In panel B, yellow strata are where shale content is less than 50% (stronger rocks).

very useful for scientific purposes, especially for non-stationary signals where the statistical properties of the signal change with time or with an increase of the measurement axis.

The primary purpose of CWT is to analyze the content within the fluctuations of a signal, e.g., $f(x)$, by using small analyzing functions in terms of waves or as more commonly called, wavelets. In particular, choosing a wavelet that is orthogonal to polynomial behavior makes the wavelet transform blind to regular behavior.

Wavelets can be a real or complex-valued function, but they must be fluctuating signals of restricted duration. Also, they must be admissible; in other words, they must be an integrable function with its average having the value of "zero" (Geurts et al., 1998). A mother wavelet function, ψ, can be represented as (Grossman and Morlet, 1984):

$$\psi_{u,s}(x) = \frac{1}{\sqrt{s}}\psi\left(\frac{x-u}{s}\right), u > 0, s \in \mathbb{R}$$

where s is the scale that determines wavelength, or frequency, and u is the shift parameter. Thus, CWT is the convolution of the signal of interest, $f(x)$, with the mother wavelet by changing its s and u parameters continuously. This process shifts and dilates the mother wavelet, generating a set of wavelets for different segments of the data. This process is mathematically expressed as:

$$\mathrm{CWT}_f(u,s) = \int_{-\infty}^{+\infty} f(x)\psi_{u,s}(x)dx = \frac{1}{\sqrt{|s|}}\int_{-\infty}^{+\infty} f(x)\psi\left(\frac{x-u}{s}\right)dx.$$

This process generates a matrix of wavelet coefficients, $\mathrm{CWT}_f(u, s)$, which is also called a scalogram, that shows the localization of frequencies at different scales and time, or depth. The wavelet coefficients are, thus, where the singularities also can be detected by analyzing the scalogram. The faster the wavelet transform coefficient decreases around a given point when the scale goes to zero, the more regular $f(x)$ is around that point (Arneodo et al., 2002). In the scalogram, points around which wavelet coefficients decay very fast when the scale decreases are uniform locations. These locations miss the abrupt changes, or singularities, that stem from formation weaknesses and composition changes that we were looking for in this work. Therefore, our attention was mostly focused around lower scale values to detect the singularities by using the mother wavelets that will be appropriate for gamma log signals. For this purpose, two mother wavelets were used following the discussion in Domingues et al. (2005). The Morlet wavelet was used for locating the range of scales (frequencies) that will host the wavelet coefficients of singularities, and the Mexican hat (second derivative of the Gaussian probability density function) was used to locate the depth of the singularities in the gamma logs of the six wells.

In addition to CWT, pointwise Hölder exponents of the gamma log signals were computed. The Hölder exponent (H) of a function $f(x)$ at point x_0 is the highest value so that $f(x)$ is Lipschitz at x_0. In other words, there exists a constant C and an nth-order polynomial $P_0(x)$ so that for all values around x_0, the following is satisfied (Humeau et al., 2007; Istas and Lang, 1997):

$$\left|f(x) - P_n(x - x_0)\right| \le C|x - x_0|^H.$$

The Hölder exponent quantifies the strength of the singularity of a signal, $f(x)$, at any point. Locally, the value of the Hölder exponent is governed by the singularities, with a higher exponent denoting a more regular function (Arneodo et al., 2002). Therefore, low values of the Hölder exponent and their locations were of more interest in this work and were used in conjunction with the CWT analyses to locate and confirm the location singularities. Pointwise Hölder exponents were computed using the method of generalized quadratic variations (GQV) proposed by Ayache and Lévy-Véhel (2004). The method estimates the Hölder exponent of a multifractional Brownian motion (mBm), sampled at i/N moments, where $i = 0, \ldots. N - 1$ using:

$$H(x_i) = \frac{1}{2\delta}\left((1-\gamma) - \frac{\log \overline{V_N}(x_i)}{\log N}\right)$$

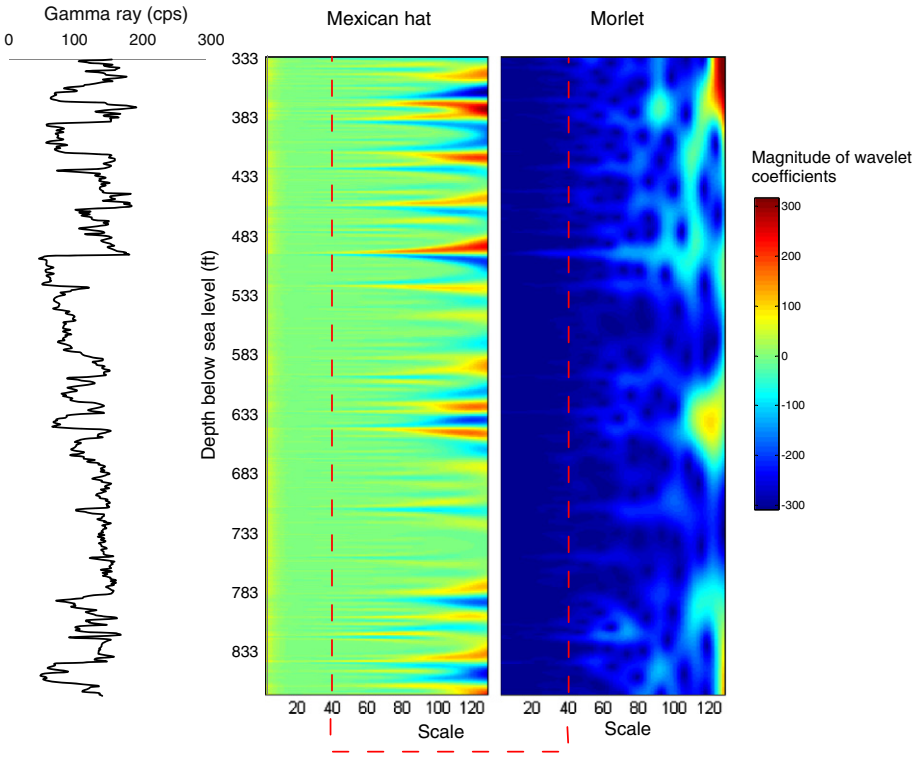

Fig. 5. Gamma log of well log 123868 and CWT coefficients maps (scalograms) using Mexican hat and Morlet mother wavelets. Dashed line indicates the scale region where singularities survive towards lower values.

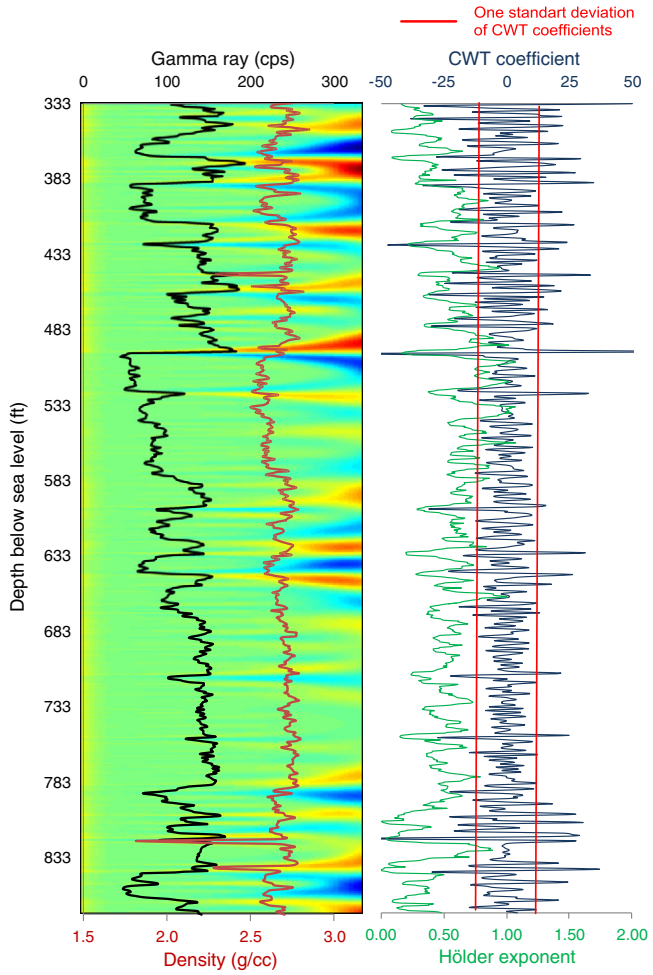

Fig. 6. Mexican hat scalogram of log 123868 overlain by gamma and density logs, shown with the wavelet coefficients at scale 40 and pointwise Hölder exponents of the gamma signal.

with the quadratic variation $\overline{V_N}(x_i)$ of a process in the neighborhood of x, with two parameters, δ and γ, which modulate $\overline{V_N}(x_i)$ in such a way that $\delta - \gamma > {}^{1}\!/_{2}$, $\gamma \geq \delta \times b$ and $0 < b < 1$.

In this work, MATLAB (2012) and FracLab v. 2.1 (2010) were used for computation and analyses of CWT and pointwise Hölder exponents by GQV.

Fig. 5 shows the gamma log and its CWT scalograms between the depth interval PR and ML of well log 123868. These scalograms were computed using Mexican hat (left) and Morlet mother wavelets (right). As seen from these maps of coefficients, the depth localization of the period changes in the gamma signal can be detected using both wavelets. However, it is also evident that these two wavelets are sensitive to different properties of the gamma logs using CWT. For instance, the Morlet wavelet provides a better localization of frequencies that correspond to uniformities or singularities, whereas the Mexican hat wavelet provides a better location of the depths that correspond to those changes. In this work, both were utilized to take advantage of their specialized properties in locating singularities.

As mentioned in the previous paragraphs, the faster the wavelet-transform coefficient decreases around a given point when the scale goes to zero, the more regular $f(x)$ is around that point (Arneodo et al., 2002). Therefore, higher wavelet coefficients at lower scales will be of more interest for locating singularities. The scalogram generated using the Morlet wavelet shows that there are three main intervals of shale–sandstone transitions along the log with high coefficient values—from the top of Fig. 5 down to about 400 ft, between 600 and 690 ft, and below 790 ft. The CWT coefficients of these intervals are prominent down to the scale value of 90. Within the high scale range above 90, it is not possible to differentiate the exact locations of the separate events that led to these coefficients. As scale decreases below 90, these high-valued regions start to diffuse out and disintegrate to individual events with high coefficients until scale 40, which can be characterized as the lower bound of the transition. Below 40, almost all events that survive with wavelet coefficients are noticeable as separate events, but without exact locations. Therefore, scale 40 was marked as the boundary where singularities actually showed up and continued to lower scale values with diminishing coefficients.

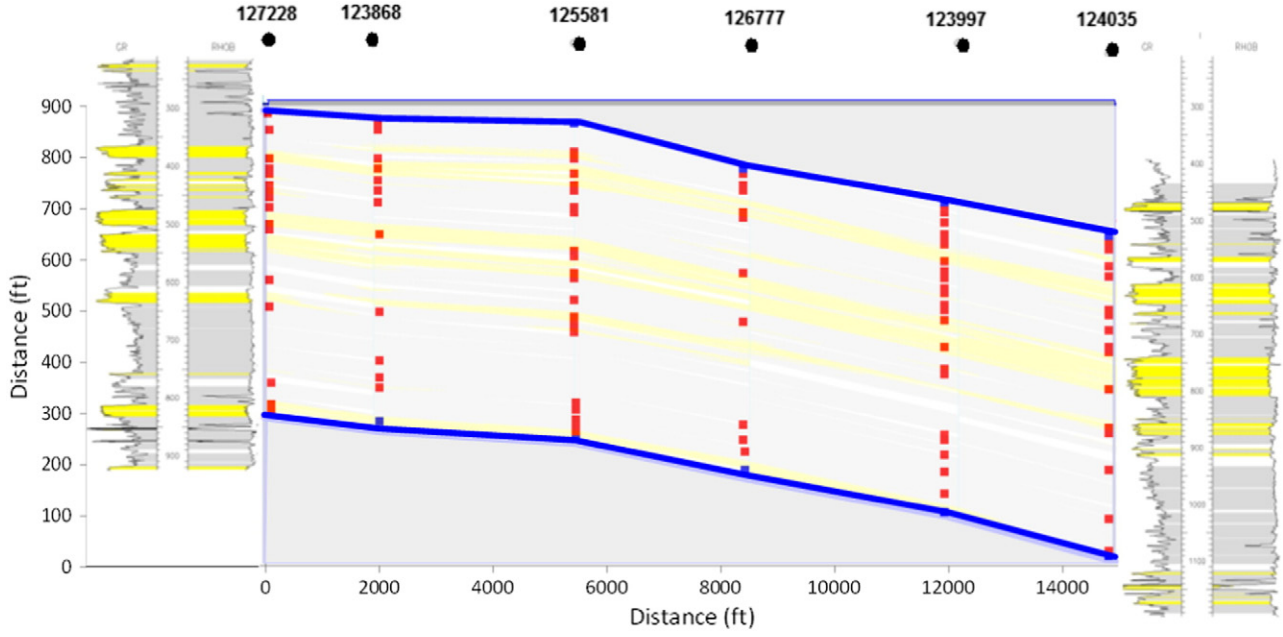

Fig. 7. Spatial locations of identified singularities (red dots) from six selected well logs and the strata correlation map within the interval of interest (PR-ML) for mining disturbances in this area. Vertical scale was expanded 10 times for viewing. In this figure, yellow strata are where shale content is less than 50%, and blue boundaries are the top of Mary Lee coal and the bottom of Pratt coals.

By comparison, the scalogram generated using the Mexican hat mother wavelet shows the depth locations of events more clearly, but without giving much information on the scale at which they should be analyzed for uniformity or singularity. Some locations are evidently uniform as far as signal changes are considered, as they disappear quickly with decreasing scale. Therefore, the scale at which the coefficients could be analyzed for their distribution in space (depth) was determined from the Morlet map, and the actual locations of potential singularities in space were determined from the Mexican hat map by extracting the coefficients at that scale. The dashed line given in Fig. 5 signifies this process. A similar approach was performed by Perez-Muñoz et al. (2013) for lithofacies characterization by parsing the scale regions of CWT scalogram to different levels.

Fig. 6 shows the scalogram generated from the gamma signal of 123868 using the Mexican hat wavelet, overlain by density and gamma log signals, as well as its coefficients retrieved at scale 40 and the pointwise Hölder exponents. As can be noticed clearly from the figure, the sharp high-magnitude variations of wavelet coefficients generally coincide with the changes in strata boundaries and other smaller-scale variations within the formations, as observed from gamma and density logs, which can be due to thin layers or local composition changes in rock layers. The locations of these variations between positive and negative values also generally coincide with the locations of the lowest values of the pointwise Hölder exponents and can be classified as locations of singularities that are of interest to this work. However, due to the fluctuating nature of the coefficient data, one standard deviation of all data points was determined (± 11.2) and the locations of the data exceeding that were considered as statistically significant ones, and marked as the locations of singularities for further analyses.

The same analyses were performed for the other five boreholes along the cross section shown in Figs. 3 and 4. For all the wellbores analyzed in this work, the occurrences of singularities were found at 27% of the total length of all boreholes within the zone of interest. The spatial locations of the identified singularities at each borehole are shown in Fig. 7, along with the strata correlation within the interval of interest. This figure shows that singularities are usually located within shale-rich formations (>50% shale) and around rocks with low shale, which are identified as sandstones and limestones in this geology, or at thin layers within those. These observations generally corroborate the empirical experiences given before and also the numerical modeling results, except for the speculations that the strata separations only occur at the weak–strong rock interfaces. Based on the spatial location of singularities, it seems likely that other intervals may be separated if subjected to mining stresses, due to various weaknesses within the formations.

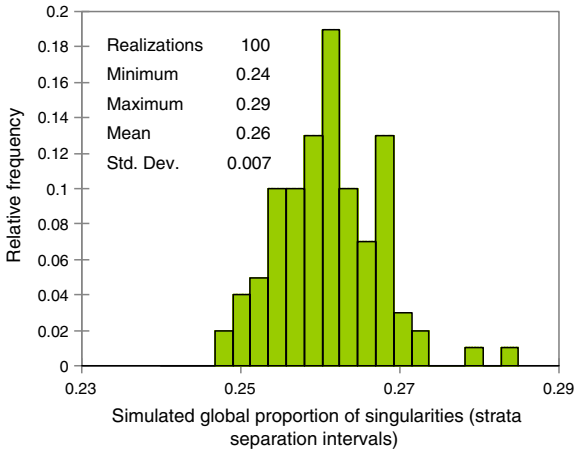

Fig. 9. Distribution of global proportions indicative of strata separation intervals resulting from 100 realizations.

Obviously identified singularities at wellbore locations will not be isolated at those very locations as far as strata separations are concerned, but will establish spatial correlation and continuity within the stratigraphic sequence. All intervals of weaknesses that will be prone to fracturing or strata separations can form a connected network of high conductivity fractures as pathways for gas migration to active or sealed zones of mines, if they are intercepted by a gas source in the overburden. Exploring the spatial continuity of identified singularities for potential strata separation intervals and their extents will be the subject of the next section.

4.3. Geostatistical modeling of identified singularities for their continuity and spatial correlation

Geostatistics is widely used for spatial correlation and continuity analyses. The theory and in-depth review of geostatistical techniques and examples are given in Deutsch and Journel (1998), Leuangthong et al. (2008), Remy et al. (2009), Olea (2009), Wackernagel (2010), and Srivastava (2013). These reviews provide the techniques and examples that mostly rely on two-point statistics and semivariograms.

Due to the limitations of two-point-based statistical techniques to model curvilinear and complex structures that are needed mostly for reservoir description, a multiple-point statistics (mps) paradigm and the use of a database, called training image (TI), was proposed by

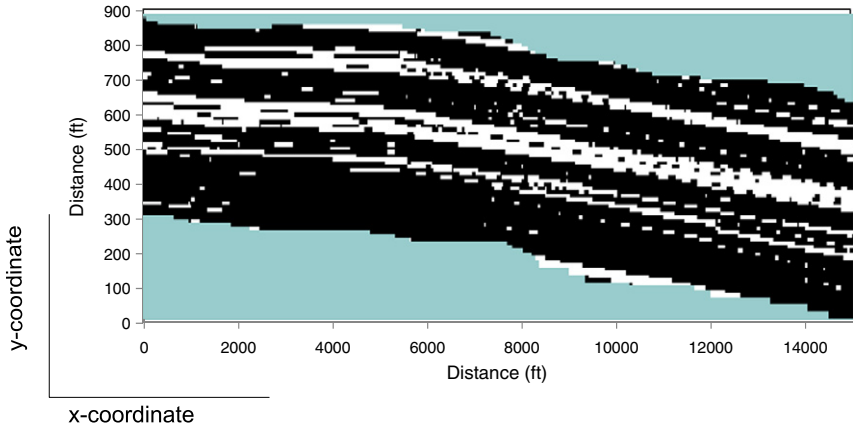

Fig. 8. The training image that was prepared and used in this work. Layers low in shale are coded as 1 (white), shale-rich regions as 0 (black), and areas not simulated as 2 (turquoise).

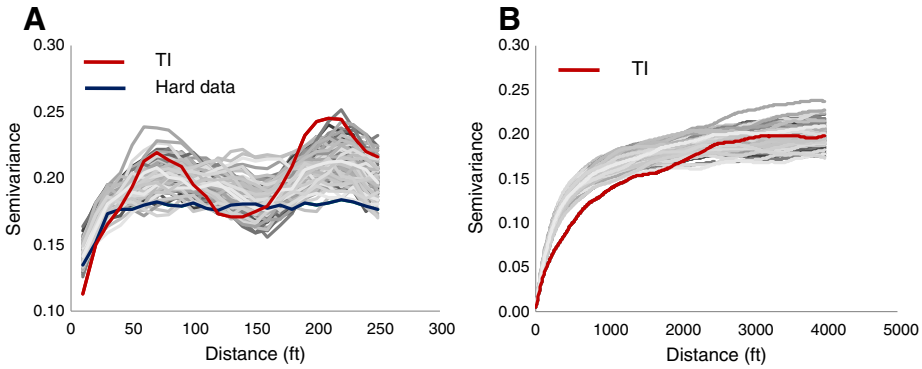

Fig. 10. Semivariograms of 100 realizations in vertical (A) and horizontal (B) directions and their comparison with those of the TI and the hard data.

Journel (1992) and extended by Guardiano and Srivastava (1992). A training image is merely a database that represents the prior geological knowledge as patterns and data, from which conditioning probability values at any multiple-point conditioning event for the pixels in simulation sequence, are determined. By the use of the TI, the mps approach was made practical with the SNESIM algorithm (Strebelle, 2000).

In this work, SGeMS (Remy et al., 2009) implementation of SNESIM was used to simulate spatial correlation and continuity of singularities within the longwall overburden shown in Fig. 7. Detailed information about SNESIM is given in Liu (2006). However, the main reasons that an mps method (SNESIM) was chosen in lieu of a semivariogram-based method were due to the known complexity of potential strata separations, and the failure in our trials to establish the horizontal component of the semivariogram that would reliably describe the heterogeneity. The latter is due to the presence of only six wells, separated by large horizontal distances when compared to vertical dimensions along the profile.

Being an mps technique, SNESIM uses a TI to represent the prior geological knowledge for collecting the pattern information needed for sequential simulation. However, it should be mentioned that in cases where the TI is generated using conceptual models, it can have its own uncertainty reflected on results. For instance, a fluvial reservoir for which the deposition environment and reservoir geometry are not well known can be a candidate for such a case. In this situation, generating multiple TIs with varying uncertainties on the prior knowledge can be considered to assess the impact of these uncertainties on results. In this work, however, the strata correlation map, which is not conceptual, was used as the TI data. The strata correlation, and thus the TI model, was generated using all density and gamma log data in CORRELATOR, which is based on minimizing the statistical uncertainty and error between correlation data points while generating a cross section. Therefore, the TI model used in this work is believed to have the least uncertainty and statistical error compared to other TIs that could have potentially been conceptualized for this purpose. To proceed further with strata correlation as the TI, the domain of interest of this image (Fig. 7) was thresholded, binarized, and formatted to conform to the same grid size and dimensions as the simulation grid, which was 1550 nodes × 10 ft, and 90 nodes × 10 ft, in horizontal and vertical directions, respectively.

The TI contained the general pattern that strata separations might exhibit. As a note, it should be mentioned that this did not have to be an exact pattern. The intention was to represent the general pattern with similar marginal probability that would be close to the target singularity proportion we wanted to simulate (0.25 versus 0.27). For this purpose, layers low in shale were coded as 1 (white), shale-rich regions as 0 (black), and the areas where there would be no simulation as 2 (turquoise). The TI used in SNESIM is shown in Fig. 8.

The SNESIM simulations were conditioned to the hard data, which were the identified singularities from previous analyses. However, there are other parameters in the program that were adjusted for their impacts on the results, as discussed by Liu (2006). The main parameters entered in the simulations and their values were: number of nodes in the search template—200; maximum, medium, and minimum ranges in the search template—5000, 10, 10 ft, respectively; angle of the template—91, 0, 0; global affinity change—2, 2, 1; minimum number of replicates—3; servosystem factor—5; number of multigrids—3; and, debug level—0.

SNESIM was used to generate 100 realizations of singularity distribution, which were identified as surrogates for intervals of strata separation with mining-induced stresses. Generating 100 realizations gave the opportunity to evaluate the uncertainty through local probabilities using all realizations through E-type map, and to select the realization that was the statistically best representation of potential strata separation intervals.

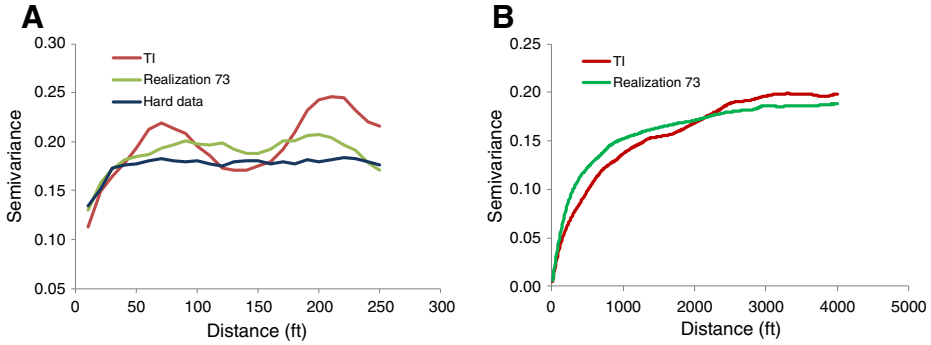

Fig. 11. Semivariograms of realization 73 in vertical (A) and horizontal (B) directions and their comparison with those of the TI and the hard data.

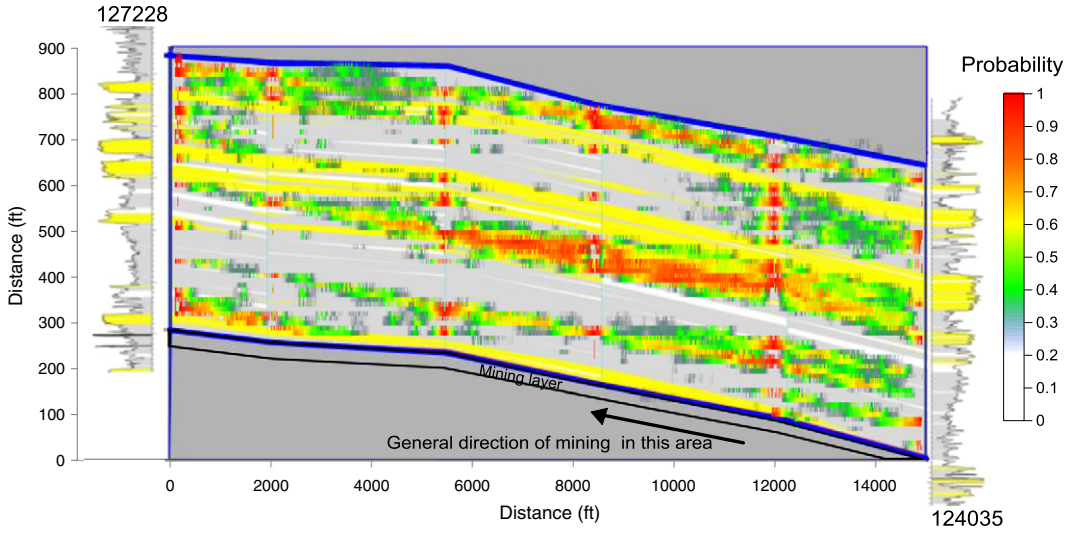

Fig. 12. E-type map of distribution and continuity of strata separation intervals shown with local probabilities. Blue boundaries are the top of Mary Lee coal and the bottom of Pratt coals.

Global proportions of the simulated distributions, which are indicative of strata separation intervals, based on 100 realizations are given in Fig. 9. The global proportion data shows that simulated values varied between 0.24 and 0.29, with a mean of 0.26. These values are close both to the proportion of the pointwise hard data, and to the global proportion extracted from the TI.

The realizations were also analyzed in terms of two-point statistics by computing their experimental semivariograms. Both horizontal and vertical semivariograms of 100 realizations were computed, along with those of the TI and with the vertical semivariogram of hard data. These data are given in Fig. 10-A and B for vertical and horizontal semivariograms, respectively. In these figures, the semivariograms that belong to hard data and the TI are shown with colored lines, and the semivariograms of all realizations are depicted as tones of gray. The semivariograms of TI and of the hard data given in Fig. 10 are placed within the semivariogram plots of 100 realizations, and thus the simulations can be considered to mimic the two-point statistics of the data and the TI in two different directions. However, there should be one realization that can represent both the TI and the hard data statistically better compared to the others.

In order to identify the realization that can represent the two-point statistics of TI and the data best, a non-parametric Kruskal–Wallis test (K–W) was applied. The K–W test helps to determine which populations are different from each other with pairwise comparisons. The pairs of populations that indicate observed differences exceeding a critical value are considered to be statistically different at the given significance level. This test creates a matrix of results indicating the pairs with statistically significant differences.

The K–W test was employed for multiple comparisons of each of the semivariogram data within each group (vertical and horizontal) separately with TI and hard data at the 0.05 significance level. The results helped to identify and to eliminate realizations that generated significantly different statistics compared to TI and hard data. This test reduced the number of candidate realizations to 25 and 27, in vertical and horizontal directions, respectively, that could further be considered. As the last step, the error between the semivariograms of these

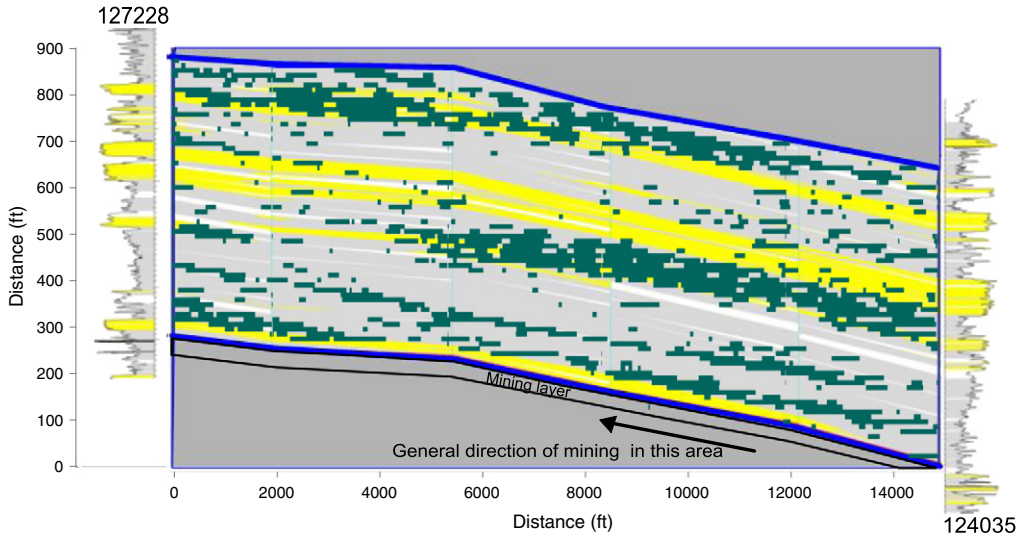

Fig. 13. Realization 73 that was determined as the statistically most representative model of the process. Green nodes represent the indicators "1" as locations of potential strata separations. In this figure, blue boundaries are the top of Mary Lee coal and the bottom of Pratt coals and yellow strata are the strong rock formations shown in Fig. 4 and in subsequent figures.

realizations and the semivariograms of TI and the hard data were calculated using the sum of squared differences approach, and the realization that gave the least error in both directions was selected.

Realization 73, which had a cumulative semivariance error of 0.0059 in the vertical direction and an error of 0.068 in the horizontal direction when compared to the TI and the data, was deemed as the best model of possible strata separation distribution in the interval of analysis. This realization also had a global proportion of 0.255 (as opposed to 0.25 of the TI and 0.27 of hard data). The semivariograms of this realization in comparison with those of TI and the hard data are shown in Fig. 11-A and B in vertical and horizontal directions, respectively.

The results can be discussed using the E-type map and realization 73, which was statistically determined as the most representative realization. The E-type map shown in Fig. 12 can be considered as the pointwise average of 100 realizations, and thus the local probability of potential strata separations.

Before discussing the results, it should be mentioned that the high probabilities at wellbore locations in the E-type map should be ignored as the runs were conditioned to the hard data, and thus it was expected that those locations would have higher probabilities. Aside from this fact, this figure shows that the probability of strata separation in the shale-rich formation above the mining horizon (ML) varies between 0.3 and 0.6, and such probabilities are observed at higher intervals and around lower-shale content rocks such as sandstones and limestone. This observation is in general agreement with the modeling and empirical results mentioned earlier. The highest probability of strata separation is observed within the shale-rich unit just below the thick sandstone sequences in the middle of the interval of interest, where the strata were dipping towards the southeast (right side of the figure). Sandstones do not seem prone to separation if there are no thin interbedded shale layers.

Fig. 13 shows realization 73 as the statistically most representative model of the strata separation process expected if the layers are subjected to mining-induced stresses. The map of indicator values shown in this figure suggests similar results with regard to separation intervals shown in E-type map, and they are also consistent with literature and field observations. Aside from the importance of these predictive results from a generic overburden response point of view, this figure and the E-type map indicate flow path locations. If these intervals are penetrated by a gas source such as an abandoned mine or gas well, gas may flow through the network of fractures in the direction of flow potential, which may be the ventilation system of the active mine.

Location of vertical fractures cannot be predicted with this method. However, Guo et al. (2012) reported, based on field measurements and geomechanical modeling, that in the fractured zone, vertical or sub-vertical and horizontal fractures are both well developed and interconnected through the layers. The thickness of this zone was postulated as 20 ft–130 ft. In this zone, both the horizontal and vertical permeabilities are high, and gas flow can occur in both directions. In the deformation zone above the fractured zone, permeability development through strata separations is more prominent. The thickness of this zone is suggested to be between 270 ft and 440 ft, calculated based on field measurements and geomechanical modeling, with much higher horizontal permeability than vertical permeability. For gas emissions into mines, the mere existence of permeable pathways may be enough. Therefore, the entire fracture and deformation interval should be considered as having potential for gas inflow, especially if there are known sources of methane along with the existence of a network of fractures for flow into the mine.

5. Summary and conclusions

The safety of coal mines and effectiveness of methane capture depend on ventilation and supplementary methane control measures. Design of these systems in turn relies on the knowledge of methane emission potential from the strata surrounding the coal mines, primarily from overburden. Strata separation intervals and the horizontal permeability that develops accordingly are major highways for gas flow within the overburden. This situation is even more important if these highly permeable fractures penetrate a methane source, which may or may not be known beforehand, and are then connected to the mine atmosphere through vertical fractures. Increased methane flow into the active or abandoned mine workings can cause serious safety and operational concerns for miners.

In this paper, a new technique to predict the potential intervals of strata separations in the longwall overburden was proposed. The technique is based on processing the commonly available drill hole gamma log signal to seek singularities that may be the precursors for strata separations when formations are exposed to mining stresses. Processing of logs was achieved using continuous wavelet transform (CWT) and generalized quadratic variations. The CWT matrix of coefficients was analyzed to locate the frequency and space parameters of singularities in the scalograms. Singularities that were isolated at their corresponding depth locations were modeled to determine their continuity and spatial correlation using multiple point geostatistical modeling with single normal equation simulation (SNESIM). The simulations generated 100 realizations to assess uncertainty and also to explore the statistically most representative case.

The results showed that the developed technique can realistically locate the intervals of strata separations consistent with the expected locations of the strata separations and data in the literature. These potential intervals are generally concentrated around the interfaces of sandstone and limestone with shale-rich formations and within shales as well. Furthermore, the separation interval probabilities and the most likely prediction of separation interval locations were presented. The proposed technique and associated results provide researchers with ability tool to predict overburden response to mining and, more importantly, the potential to predict gas flow paths into active mines.

6. Disclaimer

The findings and conclusions in this paper do not necessarily represent the views of the National Institute for Occupational Safety and Health (NIOSH). Mention of any company name, product, or software does not constitute endorsement by NIOSH or the U.S. Geological Survey.

References

Arneodo, A., Audit, B., Decoster, N., Muzy, J.-F., Vaillant, C., 2002. Wavelet based multifractal formalism: applications to DNA sequences, satellite images of the cloud structure, and stock market data. The Science of DisastersSpringer Berlin Heidelberg pp. 26–102.

Ayache, A., Lévy-Véhel, J., 2004. Identification of the pointwise holder exponent of generalized multifractional Brownian motion. Stoch. Process. Appl. 111, 119–156.

Bastante, F.G., Ordóñez, C., Taboada, J., Matias, J.M., 2008. Comparison of indicator kriging, indicator simulation and multiple-point statistics used to model slate deposits. Eng. Geol. 98, 50–59.

Briqueu, L., Zaourar, N., Laurer-Leredde, C., Hamoudi, M., 2010. Wavelet based multiscale analysis of geophysical downhole measurements: application to a clayey siliclastic sequence. J. Pet. Sci. Eng. 71, 112–120.

De Souza, L.E., Costa, J.F.C.L., 2013. Sample weighted variograms on the sequential indicator simulation of coal deposits. Int. J. Coal Geol. 112, 154–163.

Deutsch, C.V., Journel, A.G., 1998. GSLIB Geostatistical Software Library and User's Guide, 2nd edition. Oxford University Press, New York, NY (369 pp.).

Domingues, M.-O., Mendes, O., Da Costa, A.M., 2005. On wavelet techniques in atmospheric sciences. Adv. Space Res. 35, 831–842.

FracLab 2.1, 2010. A Fractal Analysis Toolbox for Signal and Image Processing. Research Center INRIA Saclay, France (http://fraclab.saclay.inria.fr/).

Gale, W., 2005. Application of computer modeling in the understanding of caving and induced hydraulic conductivity about longwall panels. Proceedings of 6th Australasian Coal Operator's Conference, Brisbane.

Gaucherel, C., 2002. Use of wavelet transform for temporal characterization of remote watersheds. J. Hydrol. 269, 101–121.

Geurts, C.P.W., Hajj, M.R., Tieleman, H.W., 1998. Continuous wavelet transform of wind and wind-induced pressures on a building in suburban terrain. J. Wind Eng. Ind. Aerodyn. 74–76, 609–617.

Groshong, R.H., Pashin, J.C., 2009. Structural controls on fractured coal reservoirs in the southern Appalachian Black Warrior foreland basin. J. Struct. Geol. 31, 874–886.

Grossman, A., Morlet, J., 1984. Decomposition of Hardy functions into square integrable wavelets of constant shape. SIAM J. Math. Anal. 723–736.
Guardiano, F., Srivastava, R.M., 1992. Multivariate geostatistics: beyond bivariate moments. In: Soares, A. (Ed.), Proceedings of the 4th International Geostatistics Congress, vol. 1. Kluwer Academic Publications, Dordrecht, Netherlands.
Guo, H., Yuan, L., Shen, B., Qua, Q., Xue, J., 2012. Mining induced strata stress changes, fractures and gas flow dynamics in multi-seam longwall mining. Int. J. Rock Mech. Min. Sci. 54, 129–139.
Hatherly, P., 2013. Overview on the application of geophysics in coal mining. Int. J. Coal Geol. 114, 74–84.
Humeau, A., Chapeau-Blondeau, F., Rousseau, D., Tartas, M., Fromy, B., 2007. Multifractality in the peripheral cardiovascular system from pointwise Holder exponents of laser Doppler flowmetry signals. Biophys. J. Biophys. Lett. http://dx.doi.org/10.1529/biophysj.119057.
Istas, J., Lang, G., 1997. Quadratic variations and estimation of the local Holder index of a Gaussian process. Ann. Inst. Henri Poincare 33, 407–436.
Journel, A.G., 1992. Geostatistics: roadblocks and challenges. In: Soares, A. (Ed.), Proceedings of the 4th International Geostatistics Congress, vol. 1. Kluwer Academic Publications, Dordrecht, Netherlands.
Karacan, C.Ö., 2009a. Reconciling longwall gob gas reservoirs and venthole production performances using multiple rate drawdown well test analysis. Int. J. Coal Geol. 80, 181–195.
Karacan, C.Ö., 2009b. Reservoir rock properties of coal measure strata of the Lower Monongahela Group, Greene County (Southwestern Pennsylvania), from methane control and production perspectives. Int. J. Coal Geol. 78, 47–64.
Karacan, C.Ö., 2013a. Production history matching to determine reservoir properties of important coal groups in Upper Pottsville formation, Brookwood and Oak Grove fields, Black Warrior Basin, Alabama. J. Nat. Gas Sci. Eng. 10, 51–67.
Karacan, C.Ö., 2013b. Integration of vertical and in-seam horizontal well production analyses with stochastic geostatistical algorithms to estimate pre-mining methane drainage efficiency from coal seams: Blue Creek seam, Alabama. Int. J. Coal Geol. 114, 96–113.
Karacan, C.Ö., Goodman, G.V.R., 2009. Hydraulic conductivity changes and influencing factors in longwall overburden determined by slug tests in gob gas ventholes. Int. J. Rock Mech. Min. Sci. 46, 1162–1174.
Karacan, C.Ö., Goodman, G.V.R., 2011. Monte Carlo simulation and well testing applied in evaluating reservoir properties in a deforming longwall overburden. Transp. Porous Media 86, 445–464.
Karacan, C.Ö., Olea, R.A., 2013. Time-lapse analysis of methane quantity in the Mary Lee group of coal seams using filter-based multiple-point geostatistical simulation. Math. Geosci. 45, 681–704.
Karacan, C.Ö., Esterhuizen, G.S., Schatzel, S.J., Diamond, W.P., 2007. Reservoir simulation-based modeling for characterizing longwall methane emissions and gob gas venthole production. Int. J. Coal Geol. 71, 225–245.
Leuangthong, O., Khan, K.D., Deutsch, C.V., 2008. Solved Problems in Geostatistics. Wiley, Hoboken (207 pp.).
Liu, Y., 2006. Using the SNESIM program for multiple-point statistical simulation. Comput. Geosci. 32, 1544–1563.
López, M., Aldana, M., 2007. Facies recognition using wavelet based fractal analysis and waveform classifier at the Oritupano-A Field, Venezuela. Nonlinear Process. Geophys. 14, 325–335.
Matlab, 2012. MathWorks, Version 2012b (Massachusetts, U.S.A.).
Olea, R.A., 2004. CORRELATOR 5.2—a program for interactive lithostratigraphic correlation of wireline logs. Comput. Geosci. 30, 561–567.
Olea, R.A., 2009. A Practical Primer on Geostatistics: U.S. Geological Survey, Open-File Report 2009-1103. http://pubs.usgs.gov/of/2009/1103/ (346 pp.).
Palchik, V., 2003. Formation of fractured zones in overburden due to longwall mining. Environ. Geol. 44, 28–38.
Palchik, V., 2005. Localization of mining-induced horizontal fractures along rock layer interfaces in overburden: field measurements and prediction. Environ. Geol. 48, 68–80.
Pan, S.-Y., Hsieh, B.-Z., Lu, M.-T., Lin, Z.-S., 2008. Identification of stratigraphic formation interfaces using wavelet and Fourier transform. Comput. Geosci. 34, 77–92.
Pashin, J.C., Carroll, R.E., McIntyre, M.R., Grace, R.L.B., 2010. Geology of unconventional gas plays in the southern Appalachian thrust belt. Guidebook for Field Trip 7, AAPG Annual Conference and Exposition, April 14–16, New Orleans, LA.
Perez-Muñoz, T., Velasco-Hernandez, J., Hernandez-Martinez, E., 2013. Wavelet transform analysis for lithological characteristics identification in siliciclastic oil fields. J. Appl. Geophys. http://dx.doi.org/10.1016/j.jappgeo.2013.09.010.
Remy, N., Boucher, A., Wu, J., 2009. Applied Geostatistics with SGeMS, A User's Guide. Cambridge University Press, Cambridge, United Kingdom (264 pp.).
Srivastava, M., 2013. Geostatistics: a toolkit for data analysis, spatial prediction and risk management in the coal industry. Int. J. Coal Geol. 112, 2–13.
Strebelle, S., 2000. Sequential Simulation Drawing Structures from Training Images. (Ph.D. Thesis) Stanford University, Stanford, CA (187 pp.).
Wackernagel, H., 2010. Multivariate Geostatistics—An Introduction with Applications, 3rd ed. Springer, Berlin (387 pp.).
Webber, T., Costa, J.F.C.L., Salvadoretti, P., 2013. Using borehole geophysical data as soft information in indicator kriging for coal quality estimation. Int. J. Coal Geol. 112, 67–75.
Whittles, D.N., Lowndes, I.S., Kingman, S.W., Yates, C., Jobling, S., 2006. Influence of geotechnical factors on gas flow experienced in a UK longwall coal mine panel. Int. J. Rock Mech. Min. Sci. 43, 369–387.